A shape-based approach for leaf classification using multiscale triangular representation

Sofiène Mouine, Itheri Yahiaoui, Anne Verroust-Blondet

▶ **To cite this version:**

A shape-based approach for leaf classification using multiscale triangular representation.

Sofiene Mouine
Inria Paris-Rocquencourt
78153 Le Chesnay, France
sofiene.mouine@inria.fr

Itheri Yahiaoui
Inria Paris-Rocquencourt
78153 Le Chesnay, France
CReSTIC Université de
Reims, FRANCE
itheri.yahiaoui@inria.fr
itheri.yahiaoui@univ-
reims.fr

Anne Verroust-Blondet
Inria Paris-Rocquencourt
78153 Le Chesnay, France
anne.verroust@inria.fr

ABSTRACT
In this paper we introduce a new multiscale shape-based approach for leaf image retrieval. The leaf is represented by local descriptors associated with margin sample points. Within this local description, we study four multiscale triangle representations: the well known triangle area representation (TAR), the triangle side lengths representation (TSL) and two new representations that we denote triangle oriented angles (TOA) and triangle side lengths and angle representation (TSLA). Unlike existing TAR approaches, where a global matching is performed, the similarity measure is based on a locality sensitive hashing of local descriptors. The proposed approach is invariant under translation, rotation and scale and robust under partial occlusion. Evaluations made on four public leaf datasets show that our shape-based approach achieves a high retrieval accuracy w.r.t. state-of-art methods.

keywords: shape descriptor, leaf image retrieval, plant identification, multiscale triangle representation, local description

1. INTRODUCTION
The large number of existing plant species in the world makes human identification of them tedious and time consuming, particularly for non-expert stakeholders such as land managers, foresters, agronomists, amateur gardeners, etc. Hence, an automatic plant identification tool should speed up the plant species identification task. This identification tool may be useful even for experienced botanists.

Plant identification is based on the observation of its organs, i.e. buds, leaves, fruits, stems, etc.. An interesting review of existing approaches developed for plant species identification can be found in [11]. A large amount of information about the taxonomic identity of a plant is contained in its leaves. This is due to the fact that leaves are present on the plants for at least several months, which is not generally the case for other organs such as fruits or flowers. Therefore, most plant identification tools based on Content-Based Image Retrieval techniques [20, 27, 5, 8, 7, 3, 9, 10] work on leaf image databases. Leaves can be characterized by their shape, color and texture. Leaf color may vary with the seasons and geographical locations. In addition, different plant species can have almost the same color leaves. Thus, color is not sufficiently discriminant to be used alone in a plant identification task.

In this paper, we focus on the shape of the leaf and on shape-based approaches for leaf recognition.

To describe the shape of a leaf, one can develop a specific approach or adapt a generic shape retrieval method to the particular case of leaves.

Specific approaches [13, 8] are based on the botanical characterization of leaf shapes. They extract morphological characters such as: Aspect Ratio, Rectangularity, Convex Area Ratio, Convex Perimeter Ratio, Sphericity, Circularity, Eccentricity and Form Factor.

Shape feature extraction techniques (cf. [26] for a survey) can be subdivided into two families: global approaches, where the shape is represented by one feature descriptor, and local approaches, where a set of local descriptors are computed at some interesting points of the shape. When global features are extracted, a global measure is used to compute the similarity of the shapes. The Curvature Scale Space approach [28] has been tested on leaves in [28, 8]. Fourier-based descriptors have also been used [41, 32, 30]. Multiscale approaches [20, 28, 2, 12, 23] have been introduced to enrich the shape description and render it more robust to noise and contour deformations.

Local approaches compute local features of landmark points of the object. Landmark points can be boundary points [6, 25] or salient points [29] of the shape. Then, a feature-to-feature matching is performed to retrieve the most similar pairs of points of two different shapes. A 2D histogram derived from the shape context [6] computing inner distances and angles between sample points of the leaf margin has been proposed in [25, 5]. Local approaches obtained good results on the Swedish leaf dataset [25] and on the Image-CLEF2011 plant identification task [29].

We want to benefit here from the advantages of both the multiscale approaches and the local ones. For this purpose,
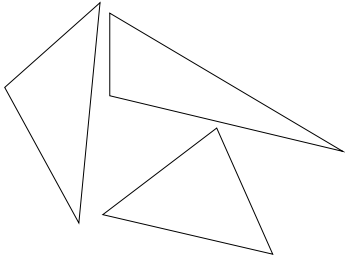
Figure 1: Three triangles having the same area

we associate a multiscale local description of the shape based on triangles to a sample of the shape contour points. Before describing our approach, let us study the possible triangle representations.

Several authors have proposed representations based on triangles built from feature points [18, 19, 36]. Tao an Grosky [36] describe the shape by a Delaunay triangulation and estimate the density of triangles discrete angles by a global histogram. In [18, 19], the authors use the angles given by the medians of the triangles, joining the labelled feature points to encode their spatial relationships.

Multiscale schemes based on triangles have been introduced to describe the contour of a shape [21, 34, 33, 14, 2]. All of them represent the triangles by their areas at each scale. Shen et al. [21] showed that the triangle area representation (TAR) is affine-invariant and proposed a fast error minimization algorithm for computing correspondence matching. El Rube et al. [14] suggested computing TAR at multiscale wavelet levels (MTAR) to reduce the noise effect on the shape boundary. More recently, Alajlan et al. [2, 1] made the triangle normalization locally for each scale and used a dynamic space warping matching to compute the optimal correspondence between two shapes.

Although TAR is affine-invariant and robust to noise and deformation, it has a high computational cost since all the boundary points are used. Moreover, TAR has two major limitations:
- The area is not informative about the type of the triangle (isosceles, equilateral, etc.) considered, which may be crucial for a local description of the boundary.
- The area is not accurate enough to represent the shape of a triangle. Figure 1 shows three triangles that are equal in area but which have different shapes.

In fact, the triangles in Figure 1 are not similar triangles. They do not fulfill any of the following three properties:
(i) All three pairs of corresponding side lengths are in the same proportion.
(ii) All three pairs of corresponding angles are the same.
(iii) Two pairs of side lengths have the same proportion and the included angle is equal.

To our knowledge, the Triangle Area Representation has not been really compared to other triangle representations (using side lengths, angles, etc.). We want here to take into account the similarity property in our triangle representation. Thus, in Section 2, we present three other triangle descriptions (TSL, TSLA and TOA), based on the triangles side lengths, their angles, or both, and integrate these representations in a multiscale based approach. Experiments are made on four public leaf datasets and presented in Section 3.
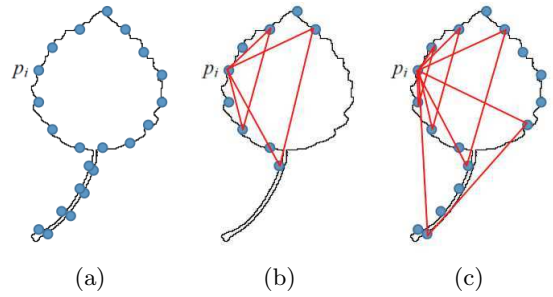

Figure 2: Multiscale triangular representation. (a) N boundary points of the leaf. Here $N = 22$. (b) N_s boundary points are selected on each side of p_i. p_i is represented by two triangles ($N_s = 2$ with $d(1) = 2$ and $d(2) = 4$) (c) p_i is represented by four triangles and logarithmic distance between triangle points ($N_s = 4$ with $d(1) = 1$, $d(2) = 2$, $d(3) = 4$ and $d(4) = 8$)

2. MULTISCALE TRIANGLE REPRESENTATION

The shape boundary is represented by a sequence of N sample points $p_1, ...p_N$ uniformly distributed over the contour and numbered in a clockwise order. Then, each contour point p_i is represented by N_s triangles computed at different scales (see Figure 2). N_s is then the number of triangles and the number of scales. Unlike other multiscale triangular representations, we introduce $d(k)$ the distance between the triangle points at scale k, expressed in the number of boundary points, with $1 \leq k \leq N_s$ and d being an increasing function such that $d(N_s) \leq N/2$. In addition, to describe p_i, we do not systematically use all the remaining boundary points. We select only two sets of N_s points on both sides of p_i. The choice of N_s depends on whether we are seeking to capture local or global information. The distance $d(k)$ may be either uniform or logarithmic (cf. Figure 2).

In what follows, each boundary point p_i is associated with N_s triangles $T_i^1, ..., T_i^{N_s}$, T_i^k being the triangle defined by the contour points $p_{i-d(k)}$, p_i and $p_{i+d(k)}$, $1 \leq k \leq N_s$.
Four triangle representations associated to each p_i are introduced:
$\text{TAR}(p_i) = (\text{TAR}(T_i^1), ..., \text{TAR}(T_i^{N_s}))$,
$\text{TSL}(p_i) = (\text{TSL}(T_i^1), ..., \text{TSL}(T_i^{N_s}))$,
$\text{TSLA}(p_i) = (\text{TSLA}(T_i^1), ..., \text{TSLA}(T_i^{N_s}))$ and
$\text{TOA}(p_i) = (\text{TOA}(T_i^1), ..., \text{TOA}(T_i^{N_s}))$.
The shape is then described by N feature vectors $\mathcal{T}(p_i); 1 \leq i \leq N$, $\mathcal{T}$ being either TAR, TSL, TSLA or TOA triangle representation. We will show that all these triangle representations are invariant to translation and rotation of the shape. By normalizing the description locally, we also obtain a scale invariant description of the shape.

2.1 Triangle area representation(TAR)

Here, for each triangle T, $\text{TAR}(T) = \mathcal{A}(T)$, where $\mathcal{A}(T)$ is the signed area of T. TAR is affine-invariant, robust to noise and provides information about local concavities or convexities at a given boundary point as the signed area is computed. Let $(x_{i-d(k)}, y_{i-d(k)}), (x_i, y_i)$ and $(x_{i+d(k)}, y_{i+d(k)})$ be the respective coordinates of the points $p_{i-d(k)}$, p_i and
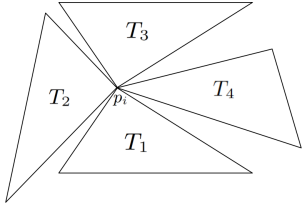
Figure 3: Three triangles having the same TSL representation

$p_{i+d(k)}$. The signed area of the triangle formed by this triplet is given by:

$$\mathcal{A}(T_i^k) = \frac{1}{2} \begin{vmatrix} x_{i-d(k)} & y_{i-d(k)} & 1 \\ x_i & y_i & 1 \\ x_{i+d(k)} & y_{i+d(k)} & 1 \end{vmatrix}$$

A normalization is made locally with respect to the maximum area in each scale as in [2]. However, the TAR used in this paper is quite different from the original TAR.
- We consider here a subset of points on the contour, unlike the original TAR where all boundary points are used.
- We define the number of scales as a parameter (N_s). In [2], $\frac{N}{2} - 1$ scales are systematically used where N is the number of points on the contour.
- The matching process is different. A dynamic space wrapping is used in [2] to compare global signatures of the shapes at each scale. Here, the feature associated to a contour point takes into account all the selected scales and then a similarity measure based on a locality sensitive hashing is used to find similar points.

2.2 Triangle side lengths representation (TSL)

TSL uses only the side lengths to represent a triangle.
Let L_{1k}, L_{2k} and L_{3k} be the three side lengths sorted in ascending order ($L_{1k} \leq L_{2k} \leq L_{3k}$) of triangle T_i^k formed by the points $p_{i-d(k)}$, p_i and $p_{i+d(k)}$, $k \in \{1, ..., N_s\}$ of the shape contour. Let $M_k = L_{1k}/L_{3k}$ and $N_k = L_{2k}/L_{3k}$. Then $\text{TSL}(T_i^k) = (M_k, N_k)$.
The three side lengths of T_i^k are proportional to M_k, N_k and 1; this is also the case for any triangle similar to T_i^k. Thus similar triangles have an equal TSL representation and TSL is invariant under scale, translation, rotation and reflection around the contour points.
Figure 3 shows an example of four triangles having the same TSL representation. T2 is a result of a rotation of T1 around p_i while T3 is the mirror image of T1 w.r.t. a horizontal line. Note that the vertex angle p_i of T_4 is different from the vertex angle p_i of the other triangles. However, the TSL representation is the same since the triangle side lengths are sorted.

2.3 Triangle represented by two side lengths and an angle (TSLA)

Let θ be the absolute value of the vertex angle at point p_i of triangle T_i^k. TSLA representation of T_i^k is the triplet (M_k, N_k, θ), where $(M_k, N_k) = \text{TSL}(T_i^k)$. TSLA is more accurate than TSL. For example, the similar triangles T_1 and
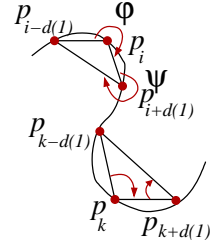
Figure 4: TOA representation

T_4 in Figure 3 have different TSLA representations because the respective angles at p_i are distinct. On the other hand, TSLA(T_1) and TSLA(T_3) are equal. Like TSL, the TSLA representation is invariant under scale and reflection around the contour points.

2.4 Triangle represented by two oriented angles (TOA)

TOA uses only angle values to represent a triangle.
Let $\phi_k = \angle p_{i-d(k)} p_i p_{i+d(k)}$ and $\psi_k = \angle p_i p_{i+d(k)} p_{i-d(k)}$ two successive oriented angles of triangle T_i^k. Then $\text{TOA}(T_i^k) = (\phi_k, \psi_k)$.
The angle orientation provides information about local concavities and convexities (cf. Figure 4). In fact, an obtuse angle means convex, an acute angle means concave. TOA is not invariant under reflection around the contour point: here, only similar triangles having equal angles at p_i will have equal TOA values.

2.5 Matching Method

TSL, TSLA and TOA represent local descriptions of contour points. In fact, a feature vector F_i is associated to each contour point p_i $i \in \{1, .., N\}$. The size of the signature using TSL, TSLA and TOA depends on the number of scales N_s.
$\text{Size}[(TSL(p_i))] = \text{Size}[(TOA(p_i))] = 2 \times N_s$.
$\text{Size}[(TSLA(p_i))] = 3 \times N_s$
$\text{Size}[(TAR(p_i))] = N_s$
When a small number of scales is used, we obtain a compact representation of each contour point. The matching process is a feature-to-feature comparison. It is the same for all the triangle descriptors presented above. The features matching is done by an approximate similarity search technique based on a Locality Sensitive Hashing (LSH) method [31]. We use the Multi Probe Locality Sensitive Hashing technique [22] and the distance L_2 to compute the similarity between two feature vectors. The principle of this algorithm is to project all the features in an L-dimensional space and to use hash functions to reduce the search and the cost time. At query time, the features $F_1, F_2, ..., F_n$ of the query image are mapped onto the hash tables and the k-nearest neighbors ($k - nn$) of each feature F_i are searched for in the buckets associated to F_i. These n lists of candidate feature matches are used as input for a voting system to rank images according to the number of matched features.

3. EXPERIMENTAL RESULTS ON LEAVES

Our descriptors have been tested on four leaf datasets: the Swedish leaf dataset[35], the Flavia dataset [38], the ImageCLEF dataset in 2011 [16] and in 2012 [17]. In all the
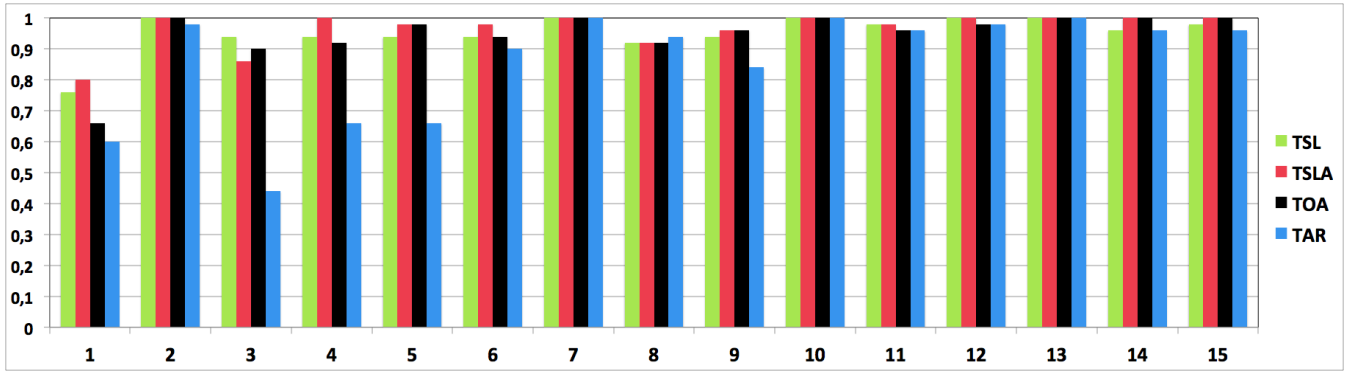
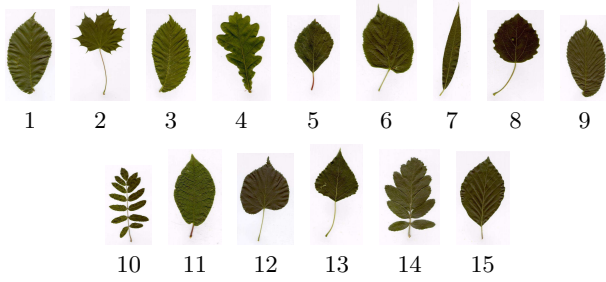Figure 5: Results per class on the Swedish leaf dataset

Figure 6: Overview of the Swedish leaf dataset. One image per species is kept.

Method	Classification rate
TSLA	**96.53%**
TSL	**95.73%**
TOA	95.20%
TAR	90.40%
Shape Tree [15]	**96.28%**
SPTC+DP[1]	95.33%
MDS+SC+DP[1]	95.33%
IDSC + DP[1]	94.13%
IDSC + learned distance [4]	93.80%
sPACT (on contour) [37]	90.77%
Fourier[1]	89.60%
SC + DP[1]	88.12%
Söderkvist [35]	82.40%

Table 1: classification rates on the Swedish leaf dataset.

experiments, a leaf image contains a single leaf on an uncluttered background. A preprocessing step is required to isolate the leaf area. First, we apply the Otsu threshold method to remove the background and keep only the mask corresponding to the leaf. A closed contour is then extracted from the leaf mask. Note that the input of all the representations described above is a sequence of N boundary points regardless of other leaf features like texture, color and venation.

3.1 The Swedish leaf dataset

The Swedish leaf dataset [35] contains 1125 images of leaves uniformly distributed in 15 species. Figure 6 shows sample leaves. The Swedish leaf dataset is very challenging because of its high inter-species similarity. One can notice the similarity of shapes of the first, third, and ninth species. To
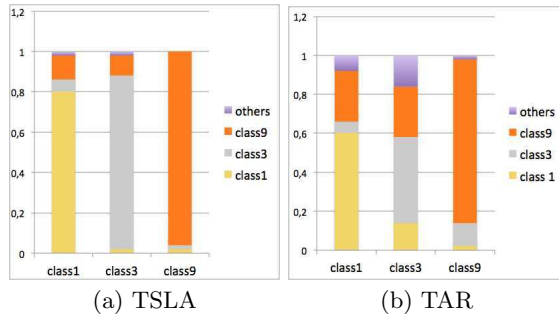

(a) TSLA   (b) TAR

Figure 7: classification results of the first, the third and the From Flaviaes

compare our approach with existing ones, we adopted the evaluation protocol used in [35, 25, 37, 4]. We randomly split each class into two sets: a training set containing 25 images and a testing set consisting of the remaining 50 images; we computed the classification rate given by the nearest neighbor (1-NN).

Table 1 shows the classification rate of the different representations compared to shape-based methods found in the literature. The number of boundary points is the same for all the proposed descriptors ($N = 400$). We are positioned first using the TSLA representation with 6 scales ($N_s = 6$) and a logarithmic periodicity between scales ($d(k) = 2^k$). TSLA outperforms all state-of-art methods while the TSL representation obtains the third best score with 95.73% using 7 scales ($N_s = 7$) and a logarithmic distance between triangles at different scales. The parameters that give the best results for the TOA and the TAR descriptors are respectively $N_s = 64$, $d(k) = 2$ x k and $N_s = 4$, $d(k) = 2^k$.

To compare the triangular representations, we use the same parameters that give the best classification rate (96.53%) with TSLA and we apply them on TSL, TOA and TAR. The performance of the descriptors for each class is shown in Figure 5. Examining the results per class on the Swedish leaf dataset, we notice that:

---

[1]methods tested in [25]

Figure 8: Sample leaves from the Flavia dataset. One image per species is shown.

- The lowest classification rates are obtained on the first class for TSL, TSLA and TOA. However, the TSLA descriptor performs better than all the other representations. This is due to the leaf shape similarity between the first, the third and the ninth classes.

Figure 7 shows that classification errors are due to the confusion between these classes. - The TSLA descriptor performs either as well as or better than the TSL descriptor on 14 out of 15 classes. This confirms our initial assumption: by adding an angle to the TSL representation, we obtain a more accurate description of the contour.

- The TSL, TSLA, TOA descriptors give higher classification rates than the TAR descriptor on 14 out of 15 classes. The difference is significant in the third, fourth and fifth class. This confirms that the triangle side lengths and angles are more informative than area about the shape of the triangle.

3.2   The Flavia dataset

The Flavia dataset is composed of 1907 scans of leaves belonging to 32 species (see Figure 8). Several methods were tested in [24] on Flavia. To compare our approach with these methods, we used the same evaluation metrics as those in [24]: the Mean Average Precision (MAP) and the recall/precision curves. The precision P and the recall R values are given by:

$$P = \frac{\#\text{relevant images}}{\#\text{retrieved images}}$$

$$R = \frac{\#\text{retrieved relevant images}}{\#\text{relevant images}}$$

The MAP value is measured on a set of queries Q and is defined as follows:

$$MAP = \frac{\sum\limits_{q \in Q} AP(q)}{|Q|}$$

where the average precision score $AP(q)$ is computed for each query q:

$$AP(q) = \frac{\sum\limits_{k=1}^{n} (P(k) \text{ x } f(k))}{\#\text{retrieved relevant images for q}}$$

$P(k)$ is the precision at cut-off k in the list of retrieved images and $f(k)$ is equal to 1 when the image at rank k is relevant and 0 otherwise. The results are reported in Table 2. The TSL, TOA, and TSLA descriptors significantly

Methods in [24]	D2	MSDM	GEDT	REM
MAP	42.82	47.91	48.01	57.21

Ours	TAR	TSL	TOA	TSLA
MAP	50.81	**65.94**	**68.37**	**69.93**

Table 2:   Mean Average Precision on the Flavia dataset
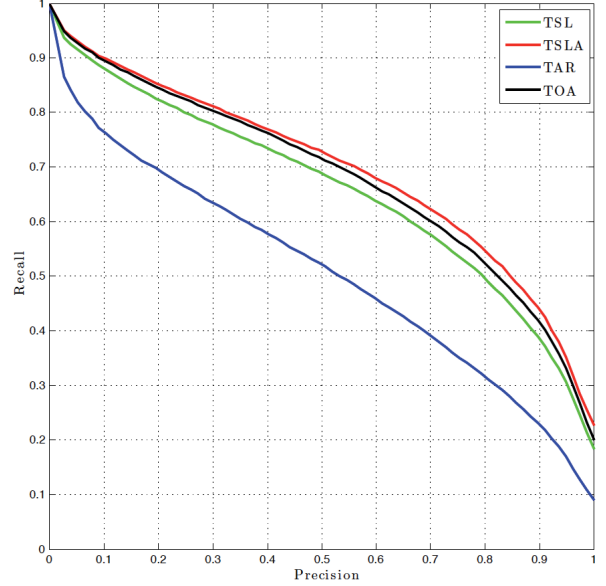
Figure 9:   Recall/Precision curves on the Flavia dataset

outperform other methods. In this experiment, we used the same parameters for all the representations: 400 boundary points and 10 scales ($N = 400$, $N_s = 10$). Despite the high similarity of the shapes of different species, our approach shows a high capability to discriminate between species.

The recall/precision curves in Figure 9 show the performance of our descriptors on the Flavia dataset. We observe that TSL, TOA, TSLA perform in a similar way. The TAR representation gives the lowest performance. The recall/precision curves also prove that the angular information (TSLA, TOA) enhances the retrieval performance.

3.3   Comparison with ImageCLEF2011 results

Let us now introduce the context of the plant identification task of ImageCLEF 2011[16]. The ImageCLEF2011 dataset contains three categories of images:
- scans of leaves acquired using a flat-bed scanner
- scan-like leaf images acquired using a digital camera
- free natural photos

For each category, the images are divided into two sets: a training set and a test set. The goal of the task is to find the correct tree species of each test image. The identification score is quite different from the classic measures such as the MAP value and recall-precision curves. Two assumptions guided the identification score S definition:
- The leaves from the same tree may be more similar than leaves from different trees (the classification rate on each

individual plant is averaged).
- Photos taken by the same person will have nearly the same acquisition protocol (S measures the mean of the average classification rate per user).
Then, S is defined as follows in ImageCLEF 2011:

$$S = \frac{1}{U} \sum_{u=1}^{U} \frac{1}{P_u} \sum_{p=1}^{P_u} \frac{1}{N_{u,p}} \sum_{p=1}^{N_{u,p}} s_{u,p,n}$$

U: number of users (who have at least one image in the test data).
P_u: number of individual plants observed by the uth user.
$N_{u,p}$: number of pictures taken of the pth plant observed by the uth user.
$s_{u,p,n}$: classification score (1 or 0) for the nth picture taken of the pth plant observed by the uth user.

We focus on scans and scan-like images. The first category contains 2349 images for training and 721 test images. For the scan-like category, 717 images are used for training and 180 images for testing. Table 4 shows the identification scores of our descriptors compared to other submitted runs of ImageCLEF2011. Our identification scores are higher than all the scores of the other methods on scans as well as scan-like images. If we average the score between the two categories, the TOA representation is slightly better. Note also that the identification score using TOA is nearly the same on scans and scan-like images, although the noise that may exist in scan-like images (shadows, cluttered background, etc.). This demonstrates that a shape-based approach is suitable for a plant identification task.

run_id	Scans	Scan-like
IFSC_USP_run2	**0.562**	0.402
inria_imedia_plantnet_run1	**0.685**	0.464
IFSC_USP_run1	0.411	0.430
LIRIS_run3	0.546	0.513
LIRIS_run1	0.539	**0.543**
Sabanci-okan-run1	**0.682**	0.476
LIRIS_run2	0.530	0.508
LIRIS_run4	0.537	**0.538**
inria_imedia_plantnet_run2	0.477	**0.554**
IFSC_USP_run3	0.356	0.187
DFH+GP [39]	**0.778**	**0.725**
TSL	**0.802**	**0.757**
TOA	**0.794**	**0.780**
TSLA	**0.796**	**0.779**
TAR	**0.721**	**0.636**

Table 3: Normalized classification scores of the scan and scan-like images on the ImageCLEF2011 dataset using the evaluation metric of [16]

3.4 Comparison with ImageCLEF2012 results

The formula used to rank the runs in the ImageCLEF2012 plant identification task [17] is nearly the same as in 2011 (see [17] for details). The scan dataset contains 4870 images for training and 1760 test images. The scan-like category contains 1819 images for training and 907 images for testing. We obtain the second best results for all the triangle descriptors on the scan images and the three descriptors TSL, TSLA and TOA outperform the ImageCLEF2012 runs for the scan-like images. Note that the method that achieved

	Scans	Scan-like
Top 3 Scores	**0.58**	**0.59**
	0.49	**0.55**
	0.47	**0.54**
TSL	**0,52**	**0.61**
TOA	**0.54**	**0.63**
TSLA	**0.53**	**0.63**
TAR	**0.52**	**0.51**

Table 4: Normalized classification scores of the scan and scan-like images using the evaluation metric of [17] (ImageCLEF2012)

the best score on scans (0.58) used a set of 27 features describing the shape, the texture and the color of the leaf [40]. In our case, we used only one shape descriptor.

3.5 Robustness to partial occlusion

In this experiment, we evaluate the performance of the proposed shape representation under partial occlusion. Partial occlusion may be due to uneven lighting conditions or overlapping objects. We picked five leaf images from the Flavia dataset and we applied three different types of occlusion: lobe occlusion, half leaf occlusion and multi occlusions. This eliminates from 20% up to 50% of the contour points. (cf. Figure 11). Taking into account that some boundary points are more sensitive to occlusion than others, we simultaneously applied multi occlusions of different parts of the leaf for the image I_5 in Figure 11.

In fact, the robustness of the descriptor depends on the choice of the number of triangles N_s. Here, the descriptor parameters are the same as those used previously on the Flavia dataset. Five retrieval tests were carried out using the occluded leaf images as queries. The results are presented in Table 5. We compare the obtained results to the scores of classification when original images are used as queries (100% for all the descriptors with $knn = 15$).

	I_1	I_2	I_3	I_4	I_5	Average	Lost
TSL	100	86.6	93.3	100	93.3	94.4	5.4
TSLA	100	100	93.3	100	60	90.6	9.4
TOA	100	100	100	100	80	96	4
TAR	93.3	86.6	80	100	73.3	86.6	13.4

Table 5: Classification rates of occluded images.

I_1 I_2 I_3 I_4 I_5
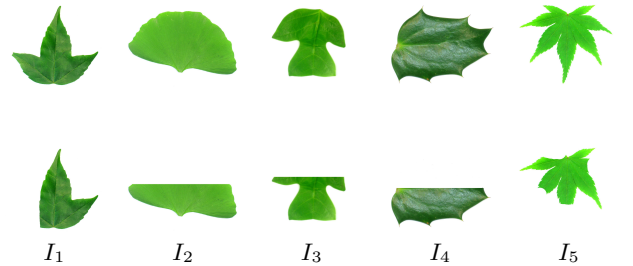
Figure 10: Partial occlusions on Flavia leaf images. First row: original images. Second row: occluded leaves

(a)

(b)
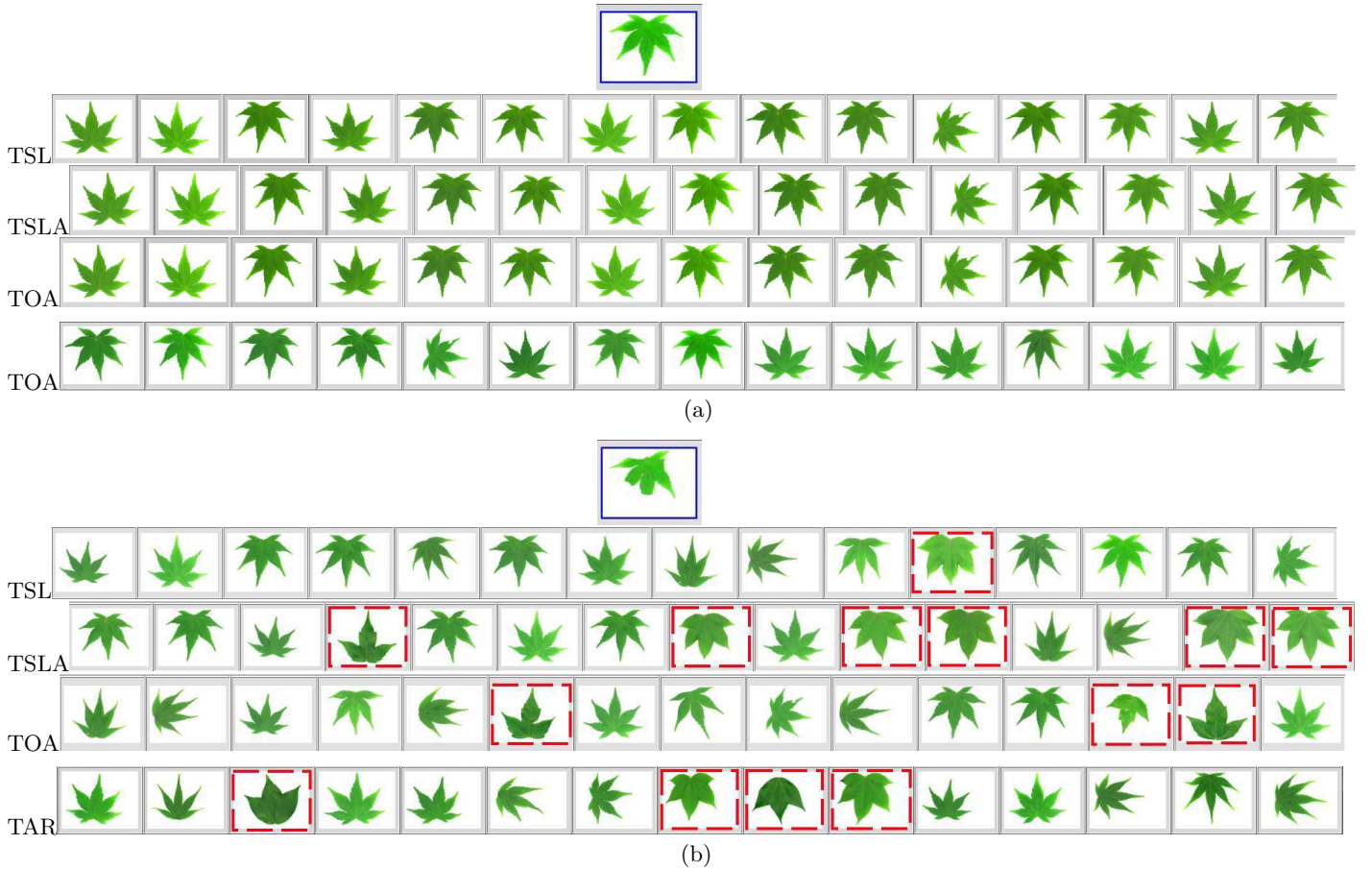
Figure 11: Examples of retrieval queries. The query image is framed by a solid blue line. False positives are framed by a dashed red line (a) the original image is used as a query image (b) the occluded image (I_5) is used as a query image

The percentage of lost information is less than 10% for TSL, TSLA and TOA. The TOA descriptor obtained the best average score of classification (96%) over the five occluded images. The TSL description is the the best in term of robustness against multi occlusions applied on the image I_5. Retrieval queries using I_5 can be seen in Figure 10.

4. CONCLUSION

In this paper, we have presented a multiscale shape-based approach for leaf classification. We have compared four triangle representations based either on area (TAR) or side lengths and angles. We have introduced two triangle representations: TSLA and TOA. The experiments carried out on four leaf datasets show that using angles and side lengths, is more appropriate than the area for triangle description. However, to compare our descriptors to the original TAR, a matching method based on dynamic programming should be developed. Moreover, the angular information provides a more precise description when it is jointly used with the triangle side lengths. Our approach is invariant to translation, rotation and scale. We have also shown that the different local descriptors are robust under partial occlusion.

In our future work, we want to include other leaf features such as venation points.

5. REFERENCES

[1] N. Alajlan, M. Kamel, and G. Freeman. Geometry-based image retrieval in binary image databases. *Pattern Analysis and Machine Intelligence, IEEE Transactions on*, 30(6):1003 –1013, june 2008.

[2] N. Alajlan, I. E. Rube, M. S. Kamel, and G. Freeman. Shape retrieval using triangle-area representation and dynamic space warping. *Pattern Recognition*, 40(7):1911 – 1920, 2007.

[3] A. R. Backes, D. Casanova, and O. M. Bruno. A complex network-based approach for boundary shape analysis. *Pattern Recognition*, 42(1):54–67, 2009.

[4] X. Bai, X. Yang, L. Latecki, W. Liu, and Z. Tu. Learning context-sensitive shape similarity by graph transduction. *Pattern Analysis and Machine Intelligence, IEEE Transactions on*, 32(5):861 –874, may 2010.

[5] P. Belhumeur, D. Chen, S. Feiner, D. Jacobs, W. Kress, H. Ling, I. Lopez, R. Ramamoorthi, S. Sheorey, S. White, and L. Zhang. Searching the world's herbaria: A system for visual identification of plant species. In *European*

Conference on Computer Vision (ECCV), pages 116–129, 2008.

[6] S. Belongie, J. Malik, and J. Puzicha. Shape matching and object recognition using shape contexts. *IEEE Transactions on Pattern Analysis and Machine Intelligence*, 24(4):509 –522, apr 2002.

[7] O. M. Bruno, R. de Oliveira Plotze, M. Falvo, and M. de Castro. Fractal dimension applied to plant identification. *Information Sciences*, 178(12):2722 – 2733, 2008.

[8] C. Caballero and M. C. Aranda. Plant species identification using leaf image retrieval. In *ACM International Conference on Image and Video Retrieval (CIVR)*, pages 327–334, 2010.

[9] D. Casanova, J. B. Florindo, and O. M. Bruno. IFSC/USP at ImageCLEF 2011: Plant identication task. In *CLEF (Notebook Papers/Labs/Workshop)*, 2011.

[10] G. Cerutti, L. Tougne, A. Vacavant, and D. Coquin. A parametric active polygon for leaf segmentation and shape estimation. In *International Symposium on Visual Computing (ISVC)*, pages 202–213, 2011.

[11] J. S. Cope, D. Corney, J. Y. Clark, P. Remagnino, and P. Wilkin. Plant species identification using digital morphometrics: A review. *Expert Systems with Applications*, 39(8):7562 – 7573, 2012.

[12] C. Direkoğlu and M. S. Nixon. Shape classification via image-based multiscale description. *Pattern Recogn.*, 44(9):2134–2146, Sept. 2011.

[13] J.-X. Du, X.-F. Wang, and G.-J. Zhang. Leaf shape based plant species recognition. *Applied Mathematics and Computation*, 185(2):883 – 893, 2007.

[14] I. El Rube, N. Alajlan, M. Kamel, M. Ahmed, and G. Freeman. Robust multiscale triangle-area representation for 2D shapes. In *Image Processing, 2005. ICIP 2005. IEEE International Conference on*, volume 1, pages I – 545–8, sept. 2005.

[15] P. F. Felzenszwalb and J. D. Schwartz. Hierarchical matching of deformable shapes. In *Computer Vision and Pattern Recognition, 2007. CVPR '07. IEEE Conference on*, pages 1–8, 2007.

[16] H. Goëau, P. Bonnet, A. Joly, N. Boujemaa, D. Barthelemy, J.-F. Molino, P. Birnbaum, E. Mouysset, and M. Picard. The CLEF 2011 plant images classification task. In *CLEF (Notebook Papers/Labs/Workshop)*, 2011.

[17] H. Goëau, P. Bonnet, A. Joly, I. Yahiaoui, D. Barthélémy, N. Boujemaa, and J.-F. Molino. The IMAGECLEF 2012 Plant identification Task. In *CLEF 2012*, Rome, Italy, Sept. 2012.

[18] D. Guru and P. Nagabhushan. Triangular spatial relationship: a new approach for spatial knowledge representation. *Pattern Recognition Letters*, 22(9):999 – 1006, 2001.

[19] N. HoĂăng, V. Gouet-Brunet, M. Rukoz, and M. Manouvrier. Embedding spatial information into image content description for scene retrieval. *Pattern Recognition*, 43(9):3013 – 3024, 2010.

[20] C. Im, H. Nishida, and T. L. Kunii. A hierarchical method of recognizing plant species by leaf shapes. In *IAPR Workshop on Machine Vision Applications (MVA)*, pages 158–161, Nov. 1998.

[21] H. H. Ip and D. Shen. An affine-invariant active contour model (ai-snake) for model-based segmentation. *Image and Vision Computing*, 16(2):135 – 146, 1998.

[22] A. Joly and O. Buisson. A posteriori multi-probe locality hashing. In *16th ACM international conference on Multimedia*, pages 209–218, 2008.

[23] N. Kumar, P. N. Belhumeur, A. Biswas, D. W. Jacobs, W. J. Kress, I. C. Lopez, and J. V. B. Soares. Leafsnap: A computer vision system for automatic plant species identification. In *12th European Conference on Computer Vision (ECCV 2012)*, pages 502–516, Florence, Italy, Oct. 2012.

[24] H. Laga, S. Kurtek, A. Srivastava, M. Golzarian, and S. Miklavcic. A riemannian elastic metric for shape-based plant leaf classification. In *Digital Image Computing: Techniques and Applications*, 2012.

[25] H. Ling and D. Jacobs. Shape classification using the inner-distance. *IEEE Transactions on Pattern Analysis and Machine Intelligence*, 29(2):286 –299, Feb. 2007.

[26] Y. Mingqiang, K. Kidiyo, and R. Joseph. A survey of shape feature extraction techniques. *Pattern Recognition Techniques, Technology and Applications*, 2008. ISBN: 978-953-7619-24-4, InTech.

[27] F. Mokhtarian and S. Abbasi. Matching shapes with self-intersections: application to leaf classification. *IEEE Transactions on Image Processing*, 13(5):653 –661, May 2004.

[28] F. Mokhtarian, S. Abbasi, and J. Kittler. Robust and efficient shape indexing through curvature scale space. In *British Machine Vision Conference (BMVC)*, 1996.

[29] S. Mouine, I. Yahiaoui, and A. Verroust-Blondet. Advanced shape context for plant species identification using leaf image retrieval. In *2nd ACM International Conference on Multimedia Retrieval*, pages 49:1–49:8, 2012.

[30] J. C. Neto, G. E. Meyer, D. D. Jones, and A. K. Samal. Plant species identification using elliptic Fourier leaf shape analysis. *Computers and Electronics in Agriculture*, 50(2):121 – 134, 2006.

[31] L. Paulevé, H. Jégou, and L. Amsaleg. Locality sensitive hashing: A comparison of hash function types and querying mechanisms. *Pattern Recognition Letters*, 31(11):1348–1358, 2010.

[32] E. Persoon and K.-S. Fu. Shape discrimination using fourier descriptors. *IEEE Transactions on Pattern Analysis and Machine Intelligence*, 8:388–397, 1986.

[33] D. Shen, H. H. Ip, and E. K. Teoh. Affine invariant detection of perceptually parallel 3d planar curves. *Pattern Recognition*, 33(11):1909 – 1918, 2000.

[34] D. Shen, W. Wong, and H. Ip. Affine-invariant image retrieval by correspondence matching of shapes, May 1999.

[35] O. J. O. Söderkvist. Computer vision classification of leaves from swedish trees. Master's thesis, Linköping University, SE-581 83 Linköping, Sweden, September 2001.

[36] Y. Tao and W. I. Grosky. Image indexing and retrieval using object-based point feature maps. *J. Vis. Lang. Comput.*, 11(3):323–343, 2000.

[37] J. Wu and J. Rehg. Where am i: Place instance and category recognition using spatial pact. In *Computer Vision and Pattern Recognition, 2008. CVPR 2008. IEEE Conference on*, pages 1 –8, june 2008.

[38] S. Wu, F. Bao, E. Xu, Y.-X. Wang, Y.-F. Chang, and Q.-L. Xiang. A leaf recognition algorithm for plant classification using probabilistic neural network. In *Signal Processing and Information Technology, 2007 IEEE International Symposium on*, pages 11 –16, dec. 2007.

[39] I. Yahiaoui, O. Mzoughi, and N. Boujemaa. Leaf shape descriptor for tree species identification. In *IEEE International Conference on Multimedia and Expo, ICME 2012*, pages 254–259, 2012.

[40] B. Yanikoglu, E. Aptoula, and C. Tirkaz. Sabanci-okan system at imageclef 2012: Combining features and classifiers for plant identification. In *CLEF (Online Working Notes/Labs/Workshop)*, 2012.

[41] C. T. Zahn and R. Z. Roskies. Fourier descriptors for plane closed curves. *IEEE Trans. Comput.*, 21(3):269–281, Mar. 1972.